Rate-Distortion Analysis of Dead-Zone Plus Uniform Threshold Scalar Quantization and Its Application—Part I: Fundamental Theory

Jun Sun, *Member, IEEE*, Yizhou Duan, Jiangtao Li, Jiaying Liu, *Member, IEEE*, and Zongming Guo, *Member, IEEE*

***Abstract*— This paper provides a systematic rate-distortion (R-D) analysis of the dead-zone plus uniform threshold scalar quantization (DZ + UTSQ) with nearly uniform reconstruction quantization (NURQ) for generalized Gaussian distribution (GGD), which consists of two aspects: R-D performance analysis and R-D modeling. In R-D performance analysis, we first derive the preliminary constraint of optimum entropy-constrained DZ + UTSQ/NURQ for GGD, under which the property of the GGD distortion-rate (D-R) function is elucidated. Then for the GGD source of actual transform coefficients, the refined constraint and precise conditions of optimum DZ + UTSQ/NURQ are rigorously deduced in the real coding bit rate range, and efficient DZ + UTSQ/NURQ design criteria are proposed to reasonably simplify the utilization of effective quantizers in practice. In R-D modeling, inspired by R-D performance analysis, the D-R function is first developed, followed by the novel rate-quantization (R-Q) and distortion-quantization (D-Q) models derived using analytical and heuristic methods. The D-R, R-Q, and D-Q models form the source model describing the relationship between the rate, distortion, and quantization steps. One application of the proposed source model is the effective two-pass VBR coding algorithm design on an encoder of H.264/AVC reference software, which achieves constant video quality and desirable rate control accuracy.**

***Index Terms*— Dead-zone plus uniform threshold quantization, generalized Gaussian distribution, rate-distortion theory, video coding.**

I. Introduction

IN DIGITAL coding realm, rate-distortion (R-D) analysis has been attracting considerable attentions. R-D analysis includes two related aspects, R-D performance analysis and R-D modeling, both are of great importance. The concept of optimal R-D performance originates from Shannon's rate-distortion function ($R(D)$) and its inverse function called the D-R function ($D(R)$) [1]. Shannon showed that when coding at rate R, the minimum distortion can arbitrarily approach the value of $D(R)$, which is only determined by the source statistics. Typically, the statistical properties of the source coefficients (also known as the memoryless sources [2]) are characterized by distributions like Gaussian [3], Laplacian [4], Cauchy [5] and the generalized Gaussian distribution (GGD) [6]. For zero-mean memoryless Gaussian source, the explicit Shannon R-D and D-R functions have already been obtained [7], denoted by $R_G(D)$ and $D_G(R)$. For zero-mean memoryless Non-Gaussian sources especially the GGD which has been proved of perfect accuracy [5]–[11] in statistical modeling, only the upper and lower bounds of the D-R function are available. The upper bound of $D(R)$ is $D_G(R)$ and the lower bound is the Shannon lower bound [2]. The D-R function of any zero-mean memoryless Non-Gaussian source lies below $D_G(R)$, while the Shannon lower bound can only be approached at very high bit rate [12]. Shannon R-D function (or D-R function) defines the best performance of all compression methods, which is obviously not applicable in practical video coding systems. Moreover, the probabilities of the real source coefficients always do not conform to Gaussian distribution. As a result, the existing explicit Shannon R-D and D-R functions $R_G(D)$ and $D_G(R)$ cannot be directly applied to video coding.

In practical video coding systems, transform-based quantization scheme is the most universal compression technology [13]. In quantization theory, the meaning of R-D function is generally extended [14] to the R-D performance of applying a certain quantization scheme such as multi-dimensional vector quantizer [15] or scalar quantizer [16] to a given source distribution. Accordingly, the attainable R-D function under applicable quantization scheme is defined as operational R-D function. Although the multi-dimensional vector quantizer can even approximate the performance of Shannon R-D function, it requires exponential computations [17] which are unbearable in application. Therefore, the simple and effective scalar quantization scheme is extensively adopted as the most suitable solution in practice. Focusing on the operational R-D function under scalar quantization scheme, a series of important achievements have been made in R-D performance analysis. The earlier contributions were mainly about the quantizer design for minimum distortion [18]–[20]. Later, considering the rate restriction in practical

Manuscript received October 12, 2011; revised May 10, 2012 and August 20, 2012; accepted August 19, 2012. Date of publication August 27, 2012; date of current version December 20, 2012. This work was supported in part by the National Natural Science Foundation of China under Contract 60902004, the National Basic Research Program of China under Contract 2009CB320907, and the Beijing Municipal Natural Science Foundation under Contract 4102025. The associate editor coordinating the review of this manuscript and approving it for publication was Prof. Ali Bilgin. *(Corresponding author: J. Liu.)*

The authors are with the Institute of Computer Science and Technology, Peking University, Beijing 100871, China (e-mail: jsun@pku.edu.cn; duanyizhou@icst.pku.edu.cn; lijiangtao@icst.pku.edu.cn; liujiaying@icst.pku.edu.cn; guozongming@icst.pku.edu.cn).

Color versions of one or more of the figures in this paper are available online at http://ieeexplore.ieee.org.

Digital Object Identifier 10.1109/TIP.2012.2215618

video communication, the optimum scalar quantizer design with output entropy rate constraint gradually became one of the hottest topics in R-D performance analysis. Among different scalar quantization schemes, the uniform threshold scalar quantizer (UTSQ) is intensively concerned for its excellent R-D performance in high bit rate. For Gaussian distribution, the optimal performance of the scalar quantizer in high bit rate was obtained using UTSQ under mean square error (MSE) distortion measure, which only exceeds Shannon R-D function by 0.255 bits/sample [21], [22]. And for various Non-Gaussian sources, UTSQ was also confirmed to be efficient [23]. In recent years, the study of scalar quantizer is further enriched by comparing UTSQ with other quantization schemes under typical distributions [24]. In addition, the dead-zone (DZ) region and the nearly uniform-reconstruction quantizer (NURQ) were introduced, which finally came into the quantization scheme of DZ + UTSQ/NURQ [25]. The performance of DZ + UTSQ/NURQ is affected by two important parameters z and f, as is shown in Fig. 1. The dead-zone ratio z is half size of the region with quantization index 0 and f is the reconstruction offset from the corresponding index. Both z and f are normalized by the quantization step Δ. DZ + UTSQ/NURQ stands for a large family of quantizers denoted by different z and f. When $z = 1$, DZ + UTSQ/NURQ degrades into UTSQ. Compared with UTSQ, DZ + UTSQ/NURQ can more flexibly adjust coding efficiency by selecting proper values of z and f. DZ + UTSQ/NURQ is nowadopted by all the major international video coding standards [26]–[31] as recommendation.

Although the integration of GGD and DZ + UTSQ/NURQ can accurately reflect the practical video coding system, to the best of our knowledge, neither the R-D property of GGD under DZ + UTSQ/NURQ nor the exact ranges of z and f for efficient DZ + UTSQ/NURQ has been obtained, indicating that further effort is required in R-D performance analysis. Taking DZ + UTSQ/NURQ design as an example, the only related work was provided by Gary [25], where the relationship of z and Δ was analyzed for Laplacian and Gaussian sources under theoretical optimal conditions. In addition, the performance comparison between uniform reconstruction quantization (URQ) and NURQ for DZ + UTSQ was provided and further extended to GGD. However, these contributions are not enough for real video applications due to the following reasons. First, there arestill no available conclusions of z to guide thedesign of efficient DZ + UTSQ/NURQ for GGD. Second, the existing results of z and f were mostly derived at very high bitrate. The restrictive condition of real coding bitrate (below 1.0 bits/sample) leads to totally different selection of z and f, which well explains why Gary's proposal of DZ + UTSQ/URQ rounding technique to H.264/AVC only effectively improves coding efficiency in very high bitrate range [25]. Besides the optimum quantizer designsolution, the knowledge of operation R-D function is also of significant importance, since it serves as the fundamental basis for R-D modeling. As a result, the lack of available R-D property of DZ + UTSQ/NURQ for GGD in the existing R-D performance analysismay bring great difficulties to the derivation of the corresponding R-D models.

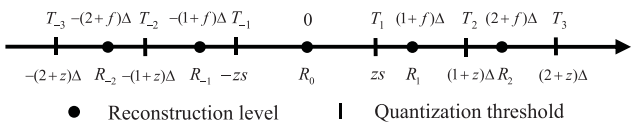

Fig. 1. Illustration of the DZ + UTSQ/NURQ scheme.

In R-D modeling, both rate and distortion of practical video coding systems are generally controlled by the quantization step under transform based quantization scheme, and the R-D function is typically characterized by the rate-quantization (R-Q) function and the distortion-quantization (D-Q) function. The R-D (or D-R), R-Q and D-Q functions together form the source model describing the relationship between rate, distortion and quantization step. By using analytical or heuristic method, several representative R-Q and D-Q models have been developed [5], [13], [32]–[37], providing useful references for video coding. However, the existing work of R-D modeling still has limitations in the following two aspects. First, for the heuristic models [34]–[37], the control parameters are determined according to the actual coding data or rate control performance. Without rigorous analysis of video source, these models can be efficient in some situations but may not effectively contribute todifferent video applications. Second, the analytical models [5], [13] are deduced base on the R-D relationship and quantization design which are applicable only in very high bit rate. As a result, these models may deviate from the practical video coding systems in actual or relatively low bit rate.

In our paper, we focus on R-D analysis of DZ + UTSQ/NURQ for GGD. The three main contributions of this paper are:

1) We rigorously demonstrate that the derivative GGD D-R function is not affected by the standard deviation β of GGD. Furthermore, we find that the derivative of GGD D-R function first decreases then increases to the traditional bound of 6.02under efficient DZ + UTSQ/NURQ patterns, which not only well explains the R-D property of GGD under DZ + UTSQ/NURQ but also simplifies the quantizer design and benefits the R-D modeling process.
2) The preliminary constraint on z and f of optimum DZ + UTSQ/NURQ for GGD is derived: $z \leq 1+f \leq z+1/2$. On this basis, z and f are further proved linear correlate in actual coding rate for GGD, and the ranges of z and f for optimal performance are also deduced, expressed as $1/2 < z \leq 1$ and $0 < f \leq 1/2$. Finally, the efficient design criteria of DZ + UTSQ/NURQ are presented by fixing f and adjusting z within the proposed range, which reasonably simplifies the implementation of effective quantizers.
3) The GGD D-R model for MPEG-4 FGS coding is extended to general DZ + UTSQ/NURQ, and the novel GGD R-Q and D-Q models under efficient DZ + UTSQ/NURQ are developed using analytical and heuristic approaches. The R-D modeling process is greatly

inspired by the R-D performance analysis, and the superior accuracy of the proposed models in estimating rate and distortion for GGD source is verified via the simulation experiments.

The remainder of this paper is organized as follows. In Section II, the DZ + UTSQ/NURQ scheme is briefly investigated and then applied to GGD to obtain the R-D property of GGD source under DZ + UTSQ/NURQ. In Section III, the relationship and the optimum ranges of z and f are derived, followed by the efficient design criteria of DZ + UTSQ/NURQ for application. The deduction and theoretical evaluation of the novel R-Q and D-Q models for GGD under efficient DZ + UTSQ/NURQ are provided in Section IV and conclusions are drawn in Section V.

II. General R-D Performance Analysis of DZ + UTSQ/NURQ With GGD

In this section, we first introduce the basic concepts of GGD and DZ + UTSQ/NURQ. Then the preliminary constraint of z and f on R-D optimized DZ + UTSQ/NURQ is derived for GGD. On this basis, detailed description is provided to illustrate the R-D property of efficient DZ + UTSQ/NURQ for GGD.

A. Zero-Mean GGD

For simplicity, we use GGD to denote zero-mean GGD in this paper. The probability density function (PDF) of GGD can be expressed as follows:

$$p(x) = \frac{g_1(\alpha)}{\beta} \exp\left(-\left[g_2(\alpha)\frac{|x|}{\beta}\right]^{\alpha}\right) \tag{1}$$

with

$$g_1(\alpha) = \frac{\alpha \cdot \Gamma(3/\alpha)^{1/2}}{2 \cdot \Gamma(1/\alpha)^{3/2}} \quad \text{and} \quad g_2(\alpha) = \left[\frac{\Gamma(3/\alpha)}{\Gamma(1/\alpha)}\right]^{1/2} \tag{2}$$

where α is the shape parameter and β is the standard deviation. Specifically, for GGD shapes $\alpha = 1.0$, $\alpha = 2.0$ and $\alpha \to \infty$, GGD becomes Laplacian, Gaussian and uniform distribution, as is shown in Fig. 2. By adjusting the parameters α and β, GGD can well adapt to the transform coefficients of various sources.

B. Preliminary Constraints of z and f

The complete DZ + UTSQ/NURQ scheme is illustrated in Fig. 1, which consists of the DZ + UTSQ *classification* rule and NURQ *reconstruction* rule, both are symmetric about zero. In classification, each input is mapped to the integer-valued quantization index according to *quantization threshold* T. In reconstruction, a real-valued *reconstruction level* R is produced for each index. For the quantization index $k \geq 1$, the decision interval is $[T_k, T_{k+1})$ and for $k \leq -1$, the interval is $(T_{-k-1}, T_{-k}]$. For the index 0, the interval is the dead-zone region given by (T_{-1}, T_1). The quantization threshold T_k and the reconstruction level R_k are expressed as:

$$T_k = \begin{cases} (k-1+z)\Delta, & k \geq 1 \\ T_{-k}, & k \leq -1 \end{cases} \quad \text{and} \quad R_k = \begin{cases} 0, & k = 0 \\ (k+f)\Delta, & k \geq 1 \\ R_{-k}, & k \leq -1. \end{cases} \tag{3}$$

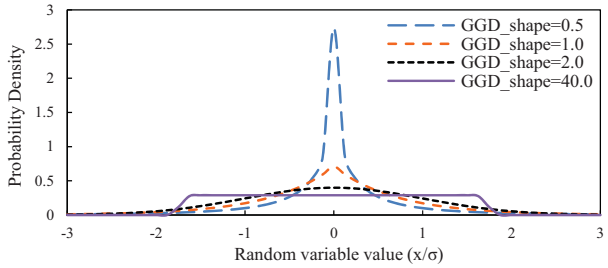

Fig. 2. Zero-mean generalized Gaussian distribution with different shape parameters.

For the symmetric quantization scheme, we first consider only *positive* axis for convenience, without loss of generality to the similar problem posed for the negative axis.

Throughout our work, we refer optimum quantizer as the one minimizes the average distortion under given limit of output entropy rate. The necessary conditions for optimum quantizer were formulated in [23], represented by the well-known conclusion from Max [18] under the mean square error (MSE) measure: for any distribution, the reconstruction level R_k should locate at the *centroid* of the PDF $p(x)$ in the decision interval $[T_k, T_{k+1})$ where $k \geq 1$. Thus the optimum DZ + UTSQ/NURQ requires that

$$R_k = \int_{(k+z-1)\Delta}^{(k+z)\Delta} xp(x)dx \Big/ \int_{(k+z-1)\Delta}^{(k+z)\Delta} p(x)dx, \qquad k \geq 1. \tag{4}$$

Since $x > 0$ and $p(x) \geq 0$, it is obvious that

$$\begin{aligned} R_k &> (k+z-1)\Delta \int_{(k+z-1)\Delta}^{(k+z)\Delta} p(x)dx \Big/ \int_{(k+z-1)\Delta}^{(k+z)\Delta} p(x)dx \\ &= (k+z-1)\Delta \end{aligned} \tag{5}$$

and

$$\begin{aligned} R_k &< (k+z)\Delta \int_{(k+z-1)\Delta}^{(k+z)\Delta} p(x)dx \Big/ \int_{(k+z-1)\Delta}^{(k+z)\Delta} p(x)dx \\ &= (k+z)\Delta. \end{aligned} \tag{6}$$

From (3), (5) and (6), the result of $z < 1 + f < z + 1$ can be directly obtained. Specifically, in some regions where $p(x) = 1$ everywhere, R_k should locate at $(z+1)\Delta$. Thus we have

$$z \leq 1 + f < z + 1. \tag{7}$$

The expression (7) is the constraint on z and f of optimum DZ + UTSQ/NURQ for all types of distributions. To refine (7) for GGD, here we first prove the important inequality of

$$\int_{(k+z-1)\Delta}^{(k+z)\Delta} xp(x)dx \leq (k+z-\frac{1}{2})\Delta \int_{(k+z-1)\Delta}^{(k+z)\Delta} p(x)dx, \quad k \geq 1. \tag{8}$$

In arbitrary positive interval $[a, b)$ we have

$$\begin{aligned}\int_a^b xp(x)dx &= \int_0^{(b-a)/2}(x+a)p(x+a)dx \\ &\quad+\int_{(b-a)/2}^{0}(b-x)p(b-x)d(b-x) \\ &= \int_0^{(b-a)/2}\big[(x+a)p(x+a) \\ &\qquad+(b-x)p(b-x)\big]dx. \end{aligned} \tag{9}$$

The PDF of GGD is monotonically decreasing in the positive axis, indicating that $[(x+a)-(b-x)][p(x+a)-p(b-x)] \le 0$ when $x \in [0,(b-x)/2]$, by which it is easy to know that $(x+a)p(x+a)+(b-x)p(b-x) \le (b-x)p(x+a)+(x+a)p(b-x)$. Therefore, we can deduce that

$$\begin{aligned}&(x+a)p(x+a)+(b-x)p(b-x) \\ &\quad\le \frac{1}{2}[(x+a)p(x+a)+(b-x)p(b-x)] \\ &\qquad+\frac{1}{2}[(b-x)p(x+a)+(x+a)p(b-x)] \\ &\quad= \frac{1}{2}(a+b)[p(x+a)+p(b-x). \end{aligned} \tag{10}$$

Using (9) and (10), the important inequality of (8) is easily proved. Then with (4) and (8), it is clear that

$$\begin{aligned}R_k &\le \left(k+z-\frac{1}{2}\right)\Delta\int_{(k+z-1)\Delta}^{(k+z)\Delta}p(x)dx\Big/\int_{(k+z-1)\Delta}^{(k+z)\Delta}p(x)dx \\ &= \left(k+z-\frac{1}{2}\right)\Delta. \end{aligned} \tag{11}$$

Finally, based on (3) and (11), the constraint of (7) is refined as:

$$z \le 1+f \le z+\frac{1}{2} \tag{12}$$

which specifies the preliminary constraint on z and f of optimum DZ + UTSQ/NURQ for GGD. In the following part of this paper, on basis of (12), the R-D property of efficient DZ + UTSQ/NURQ for GGD is concluded, and the stricter constraint of z and f are obtained for optimum quantizer design.

C. R-D Property of Efficient DZ + UTSQ/NURQ for GGD

In this subsection, we observe and analyze the property of the operational GGD D-R function under the preliminary constraint of (12) with two purposes: 1) to simplify the study of z and f for optimum DZ + UTSQ/NURQ with GGD; 2) to provide useful guidelines for R-D modeling. In [9] and [10], the R-D performance was observed for MPEG-4 FGS and H.264/SVC FGS coding, both are special instances of DZ + UTSQ/NURQ with fixed z and f. Here we extend this analysis to general DZ + UTSQ/NURQ.

With the variable $\delta > 0$, we rewrite the quantization step Δ as $\Delta_\beta = \beta\delta$. In the symmetric DZ + UTSQ classification rule, the entropy rate is calculated by the R-Q function (RQF):

$$H(\Delta_\beta) = -P_0(\Delta_\beta)\log_2 P_0(\Delta_\beta) + 2\sum_{k=1}^{+\infty} -P_k(\Delta_\beta)\log_2 P_k(\Delta_\beta) \tag{13}$$

with the probability of quantization index k

$$P_k(\Delta_\beta) = \begin{cases}\int_{-z\delta}^{z\delta} g_1(\alpha)\exp(-[g_2(\alpha)|x|]^\alpha)dx, & k=0 \\ \int_{(z+k-1)\delta}^{(z+k)\delta} g_1(\alpha)\exp(-[g_2(\alpha)|x|]^\alpha)dx, & k \ge 1.\end{cases} \tag{14}$$

For the specific shape parameter α and the constant dead-zone ratio z, it can be seen that $P_k(\Delta_\beta)$ is determined only by the variable δ. So the entropy rate is just a function of δ:

$$H(\Delta_\beta) = W_{\alpha,z}(\delta). \tag{15}$$

Likewise, in the symmetric NURQ reconstruction rule, the MSE reconstruction distortion is denoted by the D-Q function (DQF)

$$D(\Delta_\beta) = 2\sum_{k=0}^{+\infty} D_k(\Delta_\beta) \tag{16}$$

with the distortion of the kth reconstruction level

$$D_k(\Delta_\beta) = \begin{cases}\beta^2\int_0^{z\delta} x^2 g_1(\alpha)\exp(-[g_2(\alpha)|x|]^\alpha)dx, & k=0 \\ \beta^2\int_{(z+k-1)\delta}^{(z+k)\delta}[x-(f+k)\delta]^2 g_1(\alpha) \\ \quad\exp(-[g_2(\alpha)|x|]^\alpha)dx, & k \ge 1.\end{cases} \tag{17}$$

According to the equation (16) and (17), it is easy to know that for any given α, z and offset f, the distortion can also be regarded as a function of variable δ, while β only serves as a scaling factor: $D(\Delta_\beta = \beta^2 T_{a,z,f}(\delta))$. Using PSNR as the distortion measure, the DQF is expressed as

$$\begin{aligned}PSNR(\Delta_\beta) &= 10\log_{10}(255^2/D(\Delta_\beta)) \\ &= 20\log_{10}(255/\beta) - 10\log_{10} T_{a,z,f}(\delta). \end{aligned} \tag{18}$$

Normally, the RQF and DQF are combined to directly obtain the D-R function (DRF) or R-D function (RDF). Since the complex exponential expression of $W_{a,z}(\delta)$ and $T_{a,z,f}(\delta)$ cannot be simplified to derive the explicit relationship between rate and distortion, we turn to the derivative RQF and DQF. In Appendix, the existence of the derivative RQF and DQF on δ is rigorously demonstrated. Therefore, by combining the derivative functions of (15) and (18), the derivative DRF is expressed as

$$\frac{d_{PSNR(\Delta_\beta)}}{d_{H(\Delta_\beta)}} = \frac{d_{PSNR(\Delta_\beta)}/d_\delta}{d_{H(\Delta_\beta)}/d_\delta} = -\frac{10\,T'_{\alpha,z,f}(\delta)}{\ln 10\,T_{\alpha,z,f}(\delta)\,W'_{\alpha,z}(\delta)} \tag{19}$$

where $W'_{a,z}(\delta)$ and $T'_{a,z,f}(\delta)$ respectively denote the derivative function of $W_{a,z}(\delta)$ and $T_{a,z,f}(\delta)$ on δ.

Based on the derivative DRF, two important conclusions are derived. First, from (19) it is obvious that the GGD standard deviation β is not relative to the derivative DRF. Since different β only lead to the parallel displacement of the entire DRF curve, we just need to observe the R-D property of GGD with different shapes of α under DZ + UTSQ/NURQ. Second, the R-D property of GGD sources under typical DZ + UTSQ/NURQ patterns is learned from simulation experiments. Related results for $\alpha = 0.5$ and 1.0 are shown in Fig. 3, from which the derivative of the DRF can be concluded to first decrease and then increase to the traditional limitation 6.02 dB/bit with the increment

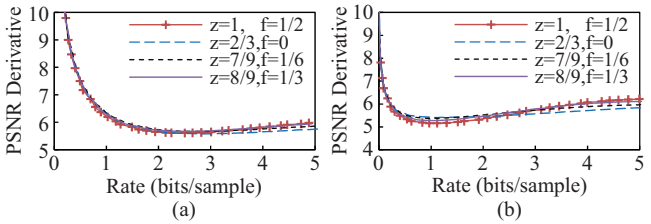

Fig. 3. D-R derivative curve of GGD under the preliminary constraint of optimum DZ + UTSQ/NURQ patterns.

of bit rate. The GGD shape α only affects the inflexion of the derivative curve, which is smaller when α is larger, with the value of 2.5 bits/sample for $\alpha = 0.5$ and 1.2 bits/sample for $\alpha = 1$. Since most actual transform coefficients are modeled using GGD with shape between 0.5 and 1.0 [8], and the practical coding rate is often below 1.0 bits/sample, it can be concluded that in real video applications where DZ + UTSQ/NURQ is implemented, the derivative of the DRF continuously decreases as the bit rate increases. It should also be noted that in Fig. 3 the R-D property of efficient DZ + UTSQ/NURQ for GGD is observed under all the patterns of z and f satisfying the preliminary constraint of (12), which indicates that this property of GGD DRF is always guaranteed under efficient DZ + UTSQ/NURQ.

In sum, the above two conclusions are important to the R-D analysis of DZ + UTSQ/NURQ for GGD. On one hand, with the first conclusion, the R-D efficiency under different patterns of z and f only need to be evaluated for typical GGD shapes without concerning the standard deviation, which effectively simplifies the quantizer design problem. On the other hand, the second conclusion describes the property of GGD DRF under efficient DZ + UTSQ/NURQ from low to high bit rate, which helps to obtain the accurate GGD D-R model in Section IV-A.

III. In-Depth Analysis of Z and F

In this section, for GGD source, we first prove that z and f of optimum DZ + UTSQ/NURQ can be effectively described as linear correlate in the real coding bit rate range. Then, the exact ranges of z and f for optimum DZ + UTSQ/NURQ are rigorously deduced. Based on this investigation, a rational solution is proposed to implement efficient DZ + UTSQ/NURQ in practice.

A. Linear Constraint of z and f

For optimum DZ + UTSQ/NURQ, the necessary condition is that the reconstruction level should locate at the centroid of the PDF in each quantization interval (see Section II-C), implying that different selections of z and f can result in similar R-D performances. It is verified that most actual transform coefficients have GGD shape α between 0.5 and 1.0 [8], and the GGD with α between 0.1 and 1.0 provides a useful model of broad-tailed process [23]. Therefore, it can be assumed that for the real source, in intervals other than the dead-zone region, the GGD PDF can be regarded linear with a slope approximating 0 which is determined by α.

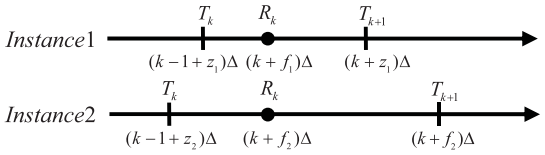

Fig. 4. Illustration of two groups of z and f that result in different DZ + UTSQ/NURQ instances with similar (optimal) R-D performance.

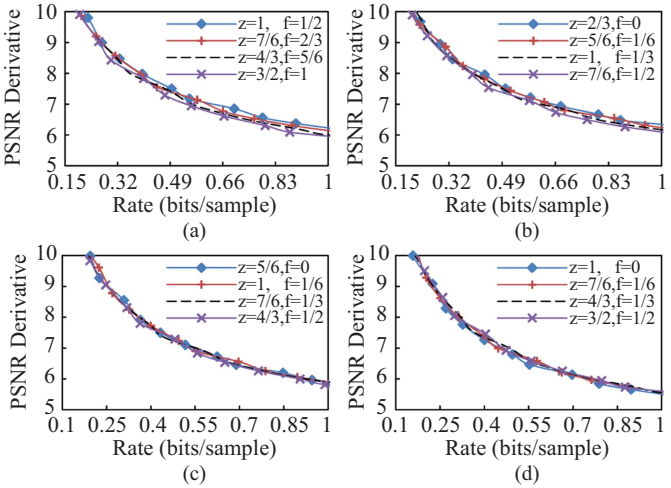

Fig. 5. D-R derivative curve of GGD shape 0.5 under the linear constraint of optimum DZ + UTSQ/NURQ in real coding bit-rate range. (a) $z - f = 1/2$. (b) $z - f = 2/3$. (c) $z - f = 5/6$. (d) $z - f = 1$.

Taking interval $[T_k, T_{k+1})$ for example, for an optimum DZ + UTSQ/NURQ instance, R_k is the centroid that divides the region into two parts $\overline{T_k R_k}$ and $\overline{R_k T_{k+1}}$, as is shown in Fig. 4. With the given α between 0.1 and 1.0, the slope of GGD PDF in $[T_k, T_{k+1})$ can be treated as fixed value, which indicates that $\overline{T_k R_k}/\overline{R_k T_{k+1}}$ should keep constant. Using z_1, f_1 and z_2, f_2 to represent two groups of different z and f, we have

$$\frac{(k+f_1)-(k-1+z_1)}{(k+z_1)-(k+f_1)} = \frac{(k+f_2)-(k-1+z_2)}{(k+z_2)-(k+f_2)}. \quad (20)$$

From (20) we can derive that $z1 - z2 = f1 - f2$, which means z and f are linear correlate. Based on the preliminary constraint of (12), the stricter linear constraint on z and f is deduced:

$$z - f = c, \qquad \frac{1}{2} \le c \le 1 \quad (21)$$

where c is constant.

Simulation experiments of the D-R derivative curves with GGD shapes 0.5 and 1.0 under the linear constraint are observed through four typical efficient DZ + UTSQ/NURQ patterns $z-f = 1/2$, $z-f = 2/3$, $z-f = 5/6$ and $z-f = 1$. The corresponding results in the real coding bit rate range are provided in Fig. 5 and Fig. 6, which shows that different DZ + UTSQ/NURQ designs conforming to the same pattern of z and p are of similar R-D performances. More specifically, the curves generated by $z-f = 1$ coincide perfectly from low to high bit rate as is exhibited in Fig. 7. And for the instances satisfying $z - f = c$ where $1/2 \le c \le 1$, the difference of the D-R derivative curves gradually accumulates as bit rate increases, from which we can conclude that under the same

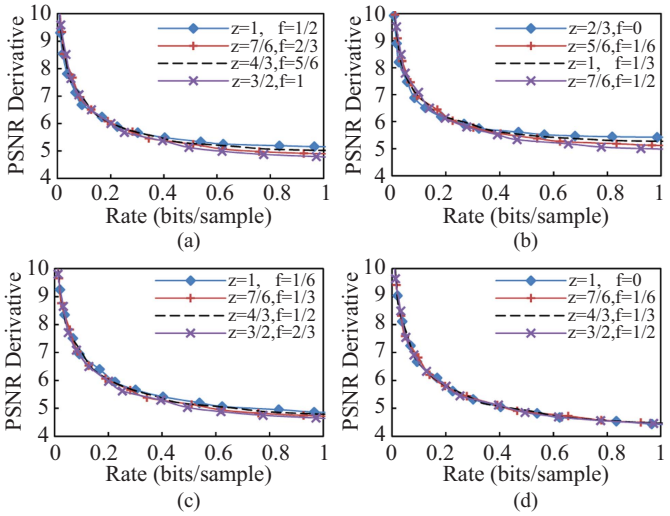

Fig. 6. D-R derivative curve of GGD shape 1.0 under the linear constraint of optimum DZ + UTSQ/NURQ in real coding bit-rate range. (a) $z - f = 1/2$. (b) $z - f = 2/3$. (c) $z - f = 5/6$. (d) $z - f = 1$.

pattern of $z - f = c$, $1/2 \le c \le 1$, the quantizer with smaller z provides better R-D efficiency.

To sum up, the linear constraint of (21) is a good approximation of the relationship between z and f in the real coding bit rate range for GGD. Different DZ + UTSQ/NURQ designs conforming to the same pattern of z and f lead to similar efficiency, thus the optimum DZ + UTSQ/NURQ design can be simplified to the selection of the DZ + UTSQ/NURQ patterns with optimal R-D performance. Since z and f are linear correlate, for convenience it is reasonable to represent each pattern of DZ + UTSQ/NURQ by fixing one of z and f and properly adjusting the other one. Therefore, the R-D comparison between different patterns can be further simplified to the observation of the R-D performance under DZ + UTSQ/NURQ where only one of z and f is adjusted. In this case, there are still two questions to be answered: 1) what are the exact ranges of z and f in which they can be fixed or adjusted; 2) how to decide which one of z and f should be fixed and which one should be adjusted. In the following two subsections we give answers to the above questions. For the first one, the optimal ranges of z and f are rigorously deduced, and for the second one, the strategy is presented by fixing f and adjusting z within the proposed range.

B. Optimal Ranges of z and f

Since the linear constraint still provides infinite ways to select z and f, it is meaningful to further excavate the exact ranges of z and f for optimum DZ + UTSQ/NURQ with GGD. In [24], for Laplacian distribution, Gary derived the range of z in the design of optimum UTSQ, known as $1/2 < z < 1$. Here we rigorously deduce a more comprehensive conclusion of z and f for optimum DZ + UTSQ/NURQ with the GGD source of actual transform coefficients in the real coding bit rate range.

First, with the linear constraint (21) and $f \ge 0$, it is easy to know $z \ge 1/2$. When $z = 1/2$, the DZ + UTSQ degrades into the special case of UTSQ, a well-known quantization scheme.

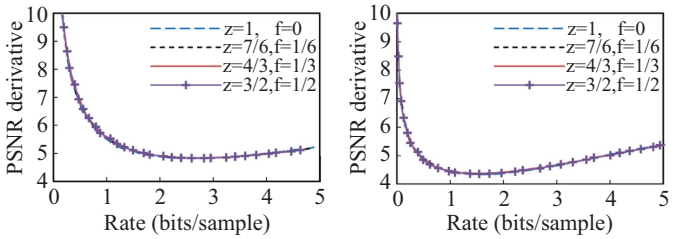

Fig. 7. D-R derivative curve for GGD under the DZ + UTSQ/NURQ pattern $z - f = 1$ from low to high bit-rate range.

In the earlier works [23], [24] and [38], UTSQ was proved optimal at very high bit rate, while in relatively lower bit rate, the requirement of infinite thresholds cannot be satisfied. Hence in real coding bit rate, UTSQ is not the choice for optimality, which refines the range of z into $z > 1/2$.

On the other hand, the NURQ degrades into the special case of URQ by fixing f to 0. More particularly, when $z = 1$ and $f = 0$ are both satisfied, URQ further degrades into uniform reconstruction with unity ratio quantizer (URURQ). URQ and URURQ are both widely used for their simplicity in design and operation. It has been verified by Gary that URURQ gives the lower bound on the performance of the best URQ [24], while URQ is proved sub-optimal for GGD [25]. Although for GGD, the R-D difference between URQ and optimum NURQ is negligible [25], to be strict, URQ is still not the choice for optimality, not to mention URURQ. Note that URURQ conforms to $z - f = 1$. Since the quantizers conforming to the pattern $z - f = 1$ with the same α are of exactly the same R-D performance, it is reasonable to use $z - f = 1$ as a benchmark of sub-optimal efficiency to evaluate other DZ + UTSQ/NURQ patterns in the real coding bit rate range. As a result, $z - f = 1$ and $f = 0$ are both excluded from the optimal ranges, making the interim result of $f > 0$ with the refined linear constraint of $z - f = c$, where $1/2 \le c < 1$.

Furthermore, the conclusion of linear constraint shows that, under the same quantization pattern of $z - f = c$, $1/2 \le c < 1$, the better R-D performance is obtained by the quantizer with smaller z. Thus, for any $z > 1$ we can find a new value of $z^* \le 1$ and the corresponding f^* satisfying $z^* - f^* = c$ with better R-D efficiency. Therefore, the optimal performance is achieved only when $z \le 1$, which also implicates that $f \le 1/2$.

Through above rigorous deduction, we finally derive the optimal ranges of z and f for DZ + UTSQ/NURQ with GGD source of actual transform coefficients:

$$\frac{1}{2} < z \le 1 \tag{22}$$

and

$$0 < f \le \frac{1}{2} \tag{23}$$

under the linear constraint of (21).

C. Efficient DZ + UTSQ/NURQ Design for Practice

The optimum ranges have provided an acceptable scope to decide the values of z and f. However, in video coding application, different standards support different proposals of

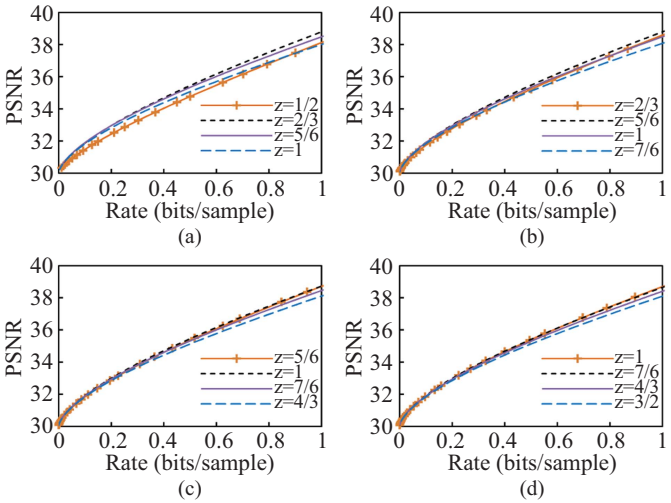

Fig. 8. D-R derivative curve of GGD shape 0.5 under the linear constraint of optimum DZ + UTSQ/NURQ in real coding bit-rate range. (a) $f = 0$. (b) $f = 1/6$. (c) $f = 1/3$. (d) $f = 1/2$.

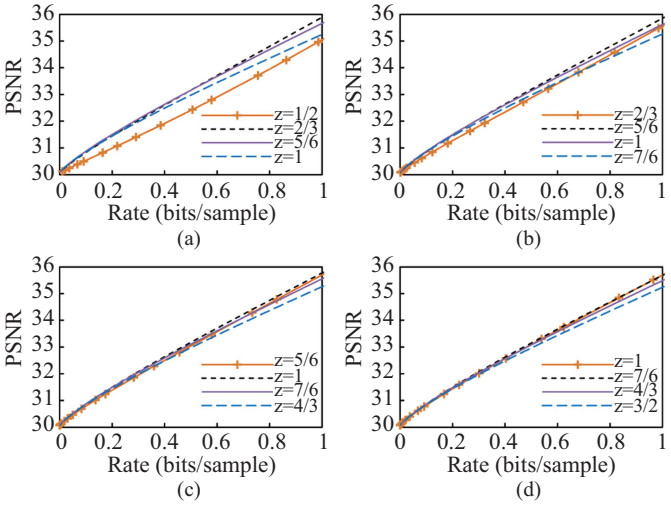

Fig. 9. D-R derivative curve of GGD shape 1.0 under the linear constraint of optimum DZ + UTSQ/NURQ in real coding bit-rate range. (a) $f = 0$. (b) $f = 1/6$. (c) $f = 1/3$.(d) $f = 1/2$.

setting f for quantization [25], which still causes confusion. To inspire a rational solution of efficient DZ + UTSQ/NURQ design for practice, we carefully analyze the D-R curves of GGD in the real coding bit rate range through two groups of simulation experiments.

The first group of experiments is designed to evaluate the influence of z on R-D performance. For GGD shapes α between 0.5 and 1.0, four f values 0, 1/6, 1/3 and 1/2 are selected, each generating four D-R curves from four DZ + UTSQ/NURQ linear patterns: $z-f = 1/2$, $z-f = 2/3$, $z-f = 5/6$ and $z-f = 1$. In this way, z is the only variable to affect R-D performance. The results for $\alpha = 0.5$ and $\alpha = 1.0$ are illustrated in Fig. 8 and Fig. 9 respectively, and the important conclusions referred in our previous analysis are also verified. First, the UTSQ represented by $z = 1/2$ is shown in Fig. 8(a) and Fig. 9(a), which is of explicitly poor performance in the real coding bit rate range. Second, Fig. 8 and Fig. 9 illustrate the R-D comparison between $z - f = 1$ and other patterns, confirming that the optimum DZ + UTSQ/NURQ

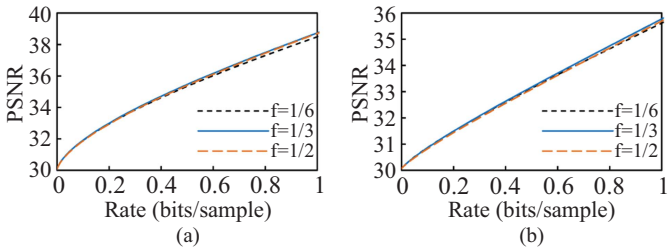

Fig. 10. D-R curves of GGD under three different patterns of optimum DZ + UTSQ/NURQ in real coding bit-rate range. (a) $\alpha = 0.5$ and $z = 1$. (b) $\alpha = 1.0$ and $z = 1$.

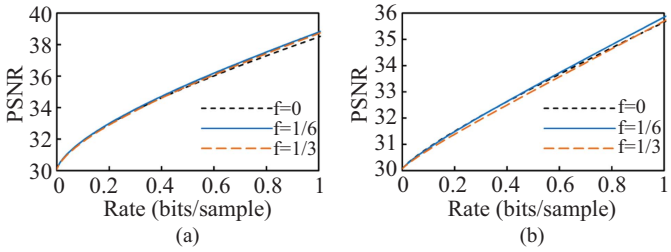

Fig. 11. D-R curves of GGD under three different patterns of optimum DZ + UTSQ/NURQ in real coding bit-rate range. (a) $\alpha = 0.5$ and $z = 5/6$. (b) $\alpha = 1.0$ and $z = 5/6$.

patterns should at least outperform the benchmark of URURQ. The first group of experiments well demonstrates that the R-D performance is greatly affected by the selection of z. The superiority in R-D performance is observed only when z approaches the optimal range of (22). Thus, to achieve the best coding efficiency, it is necessary to keep z within the optimal range as the most important prerequisite.

The second group of experiments is designed to evaluate the influence of f on optimal R-D performance, which is further divided into two parts. The former part observes the R-D difference of various p within the optimal range of (23), while the latter one is for the evaluation of URQ ($f = 0$). In each part, D-R curves generated by three patterns $z - f = 1/2$, $z - f = 2/3$, $z - f = 5/6$ are exhibited for GGD shapes $\alpha = 0.5$ and $\alpha = 1.0$. To keep optimality, z is required to be within the range of (22). For convenience, we fix z to 1 in the former part and 5/6 in the latter one. Corresponding results are illustrated in Fig. 10 and Fig. 11 for the two parts respectively. from which it is explicit that for the same z, different f satisfying (23) result in very similar R-D performances. In addition, Fig. 11 shows that the R-D difference between optimum DZ + UTSQ/NURQ and URQ is also unnoticeable in the real coding bit rate range. The second group of experiments implies that in real coding bit rate range, when z is within the optimum range, different f from $0 \le f \le 1/2$ actually will not affect the optimality of coding efficiency.

In the end, with all the above analysis and experiments, the efficient DZ + UTSQ/NURQ design criteria for practice are formed. Normally, we can fix f to an arbitrary value satisfying the optimal range $0 < f \le 1/2$ and merely adjust z within the range $1/2 < z \le 1$ to achieve optimal R-D performance. For the simplicity of operation in practice, we can also choose URQ by simply setting f to 0. In this

case, we need to keep z in the range of $1/2 < z < 1$ to avoid URURQ and obtain nearly-optimal coding efficiency. The convenience and effectiveness of URQ are the most important reason of its prevalence in the latest video coding standard H.264/AVC. In sum, with our proposed solution, the implementation of efficient DZ + UTSQ/NURQ is effectively and reasonably simplified in practice.

IV. R-D Modelingof GGD Under DZ + UTSQ/NURQ

Guided by the R-D performance analysis in Section II and III, in this section, a heuristic D-R model is first developed. Then we theoretically deduce the novel R-Q and D-Q models of GGD under DZ + UTSQ/NURQ using analytical and heuristic methods. Simulation experiments are provided to verify the excellence of the proposed models compared with other representative R-Q and D-Q models.

A. Proposed R-D Model of DZ + UTSQ/NURQ for GGD

As we have concluded in Section II-C, the derivative DRF of DZ + UTSQ/NURQ for GGD keeps decreasing in the real coding bit rate range, which is consistent with our prior R-D analysis under MPEG-4 FGS coding [9]. Therefore, our heuristic D-R model in [9] under PSNR distortion measure can be extended to DZ + UTSQ/NURQ scheme as a more universal conclusion:

$$PSNR(R) = aR + A - (A - B)/(1 + bR). \tag{24}$$

In this D-R model, R is the bit-rate, B is the PSNR when $R = 0$, (which is also known as the distortion of the starting point in D-R curve calculated by the variance of the input signals), α and A are the asymptote parameters, b is a parameter controlling the approach of the actual D-R function to the asymptote. In the second part of the whole work, this model is rigorously validated by the actual coding experiments under the quantization scheme of H.264/AVC and is used to help design the novel two-pass method for H.264/AVC.

B. Proposed R-Q Model of DZ + UTSQ/NURQ for GGD

Since the exponential RQF of GGD formulated in (15) cannot be directly simplified, we composite the analytical and heuristic approaches to give a precise approximation of the RQFof DZ + UTSQ/NURQ for GGD. First, the RQF for GGD shape $\alpha = 1.0$ (Laplacian distribution) is theoretically deducedunder DZ + UTSQ/NURQ. Then the Laplacian result is reasonably extended to cover other GGD cases with α and β introduced, implying the interrelation between the general and special forms of GGD sources. The PDF of GGD shape $\alpha = 1.0$ (Laplacian distribution) can be expressed as

$$p(x) = \frac{\mu}{2} e^{-\mu|x|} \tag{25}$$

with the standard deviation $\beta = \sqrt{2}/\mu$. For Laplacian distribution, from (14) the probability of quantization index k under DZ + UTSQ classification rule is obtained as:

$$P_k(\Delta) = \begin{cases} \int_{-z\Delta}^{z\Delta} p(x)dx = 1 - e^{-z\mu\Delta}, & k = 0 \\ \int_{(z+k-1)\Delta}^{(z+k)\Delta} p(x)dx & \\ \quad = \frac{1}{2} e^{-(z+k-1)\mu\Delta}(1 - e^{-\mu\Delta}), & k \geq 1. \end{cases} \tag{26}$$

According to equation (13), the entropy rate is calculated:

$$\begin{aligned} H(\Delta) &= -P_0(\Delta)\log_2 P_0(\Delta) \\ &\quad -(1-e^{-\mu\Delta})\log_2\left[\tfrac{1}{2}(1-e^{-\mu\Delta})\right]\sum_{k=1}^{+\infty} e^{-(z+k-1)\mu\Delta} \\ &\quad +(1-e^{-\mu\Delta})\log_2 e \sum_{k=1}^{+\infty}\left[(z+k-1)\mu\Delta e^{-(z+k-1)\mu\Delta}\right] \\ &= -P_0(\Delta)\log_2 P_0(\Delta) \\ &\quad -\left[(1-e^{-\mu\Delta})e^{-(z-1)\mu\Delta}\log_2\left[\tfrac{1}{2}(1-e^{-\mu\Delta})\right]\right]\sum_{k=1}^{+\infty} e^{-k\mu\Delta} \\ &\quad +\left[\mu(z-1)\Delta(1-e^{-\mu\Delta})e^{-(z-1)\mu\Delta}\log_2 e\right]\sum_{k=1}^{+\infty} e^{-k\mu\Delta} \\ &\quad +\left[(1-e^{-\mu\Delta})e^{-(z-1)\mu\Delta}\log_2 e\right]\sum_{k=1}^{+\infty} k\mu\Delta e^{-k\mu\Delta} \\ &= -(1-e^{-\mu\Delta})\log_2(1-e^{-\mu\Delta}) \\ &\quad -\left[(1-e^{-\mu\Delta})e^{-(z-1)\mu\Delta}\log_2\left[\tfrac{1}{2}(1-e^{-\mu\Delta})\right]\right]\sum_{k=1}^{+\infty} e^{-k\mu\Delta} \\ &\quad +\tfrac{1}{\ln 2}\left[(z-1)\mu\Delta(1-e^{-\mu\Delta})e^{-(z-1)\mu\Delta}\right]\sum_{k=1}^{+\infty} e^{-k\mu\Delta} \\ &\quad +\tfrac{1}{\ln 2}\left[(1-e^{-\mu\Delta})e^{-(z-1)\mu\Delta}\right]\sum_{k=1}^{+\infty} k\mu\Delta e^{-k\mu\Delta}. \end{aligned} \tag{27}$$

By simple accumulation of the infinite series, it is easy to prove the following results:

$$\sum_{k=1}^{+\infty} e^{-k\mu\Delta} = \frac{e^{-\mu\Delta}}{1-e^{-\mu\Delta}} \text{ and } \sum_{k=1}^{+\infty} k\mu\Delta e^{-k\mu\Delta} = \frac{\mu\Delta e^{-\mu\Delta}}{(1-e^{-\mu\Delta})^2}. \tag{28}$$

Using (27) and (28), the RQF of DZ + UTSQ/NURQ for Laplacian sources is obtained as:

$$\begin{aligned} H(\Delta) &= e^{-z\mu\Delta} - \ln(1-e^{-z\mu\Delta})/\ln 2 \\ &\quad +\mu\Delta e^{-z\mu\Delta}(z + e^{-\mu\Delta} - ze^{-\mu\Delta})/\left[(1-e^{-\mu\Delta})\ln 2\right]. \end{aligned} \tag{29}$$

In particular, when $z = 1$, (29) is further simplified as:

$$\begin{aligned} H(\Delta) &= e^{-\mu\Delta} - \ln(1-e^{-\mu\Delta})/\ln 2 \\ &\quad +\mu\Delta e^{-\mu\Delta}/\left[(1-e^{-\mu\Delta})\ln 2\right]. \end{aligned} \tag{30}$$

which is the RQF we obtained in [9] for Laplacian source under MPEG-4 FGS coding.

Laplacian distribution is an important special case of GGD with shape $\alpha = 1.0$ and standard deviation $\beta = \sqrt{2}/\mu$. It is observed from the GGD PDF that apart from in the gamma function $\Gamma(\cdot)$, α only appears as the exponential part of the input variable. Heuristically, by introducing α and β to extend the Laplacian RQF to various GGD sources, we can rewrite $\mu\Delta$ of (29) into $(\sqrt{2}\Delta/\beta)^\alpha$ or $\sqrt{2}\Delta^\alpha/\beta$. Note that with an arbitrary variable $\delta > 0$ satisfying $\delta = \Delta/\beta$, the RQF for GGD is only a function of δ and is not related to β (see Section II-C). Therefore, it is reasonable to use $(\sqrt{2}\Delta/\beta)^\alpha$ rather than $\sqrt{2}\Delta^\alpha/\beta$ to replace $\mu\Delta$ so that the GGD R-Q model is consistent with our deduction. Thus, (29) is changed into

$$\begin{aligned} H(\Delta) &= -\frac{\ln(1-e^{-z(\sqrt{2}\Delta/\beta)^\alpha})}{\ln 2} + e^{-z(\sqrt{2}\Delta/\beta)^\alpha} \\ &\quad +\frac{(\sqrt{2}\Delta/\beta)^\alpha e^{-z(\sqrt{2}\Delta/\beta)^\alpha}(z + e^{-(\sqrt{2}\Delta/\beta)^\alpha} - ze^{-(\sqrt{2}\Delta/\beta)^\alpha})}{\left[\ln 2(1-e^{-(\sqrt{2}\Delta/\beta)^\alpha})\right]}. \end{aligned} \tag{31}$$

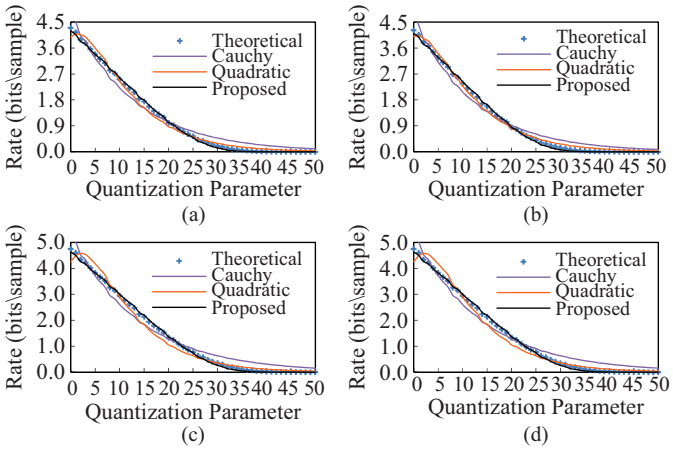

Fig. 12. Comparison of different R-Q models with the theoretical GGD rate obtained under two efficient DZ + UTSQ/NURQ patterns with GGD shape 0.5. (a) $\beta = 6$ and $z = 2/3$. (b) $\beta = 6$ and $z = 5/6$. (c) $\beta = 8$ and $z = 2/3$. (d) $\beta = 8$ and $z = 5/6$.

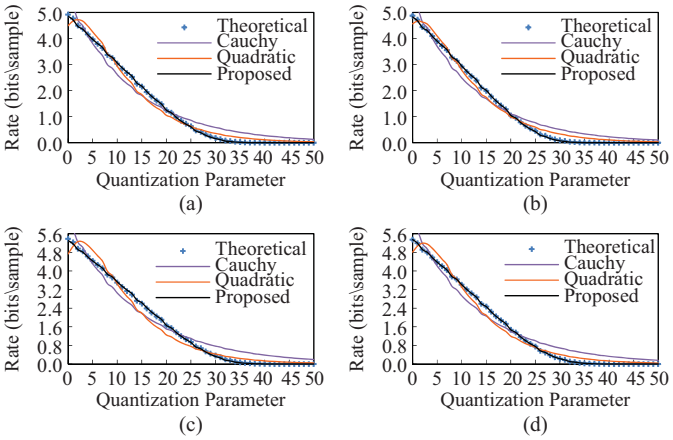

Fig. 13. Comparison of different R-Q models with the theoretical GGD rate obtained under two efficient DZ + UTSQ/NURQ patterns with GGD shape 1.0. (a) $\beta = 6$ and $z = 2/3$. (b) $\beta = 6$ and $z = 5/6$. (c) $\beta = 8$ and $z = 2/3$. (d) $\beta = 8$ and $z = 5/6$.

Equation (31) is the proposed R-Q model of DZ + UTSQ/NURQ for GGD, providing the support for different GGD parameters and dead-zone ratios to adapt to various sources and quantization settings.

To confirm the effectiveness of our finding, the theoretical GGD rate is used to evaluate different R-Q models under DZ + UTSQ/NURQ. The theoretical rate is simulated using (13) and (14), where efficient DZ + UTSQ/NURQ design with z conforming to (22) is applied. GGD shape α is chosen from 0.5 to 1.0 and β is set between 2 and 10 to conform to the statistics of actual transform coefficients [9], [10], [39]. Therefore, the theoretical GGD rate can well reflect the entropy rate of the stationary source in the practical video coding systems. For comparison, the Cauchy R-Q model [5] and the quadratic R-Q model [34] are selected to represent the analytical and heuristic methods respectively. The corresponding expressions are $H_c(\Delta) = a_c \Delta^{-ac}$ and $H_q(\Delta) = a_q \Delta^{-1} + b_q \Delta^{-2}$, where a_c, α_c and a_q, b_q are the model parameters. And we also compare with the separable R-Q model $H_s(\Delta)C(a_s \Delta^{-1} + b_s \Delta^{-2})$ [37]. For each model, the non-linear data fitting method is employed and the quantization step ranges from 0.625 to 208, corresponding to the quantization parameter of H.264/AVC from 0 to 50. Note that the separable R-Q model has similar expression to the quadratic model, for simplicity we use the results of the quadratic R-Q model to well represent the results of the separable model since the quadratic and the separable R-Q models have completely overlapping curves. Related results are illustrated in Fig. 12 and Fig. 13 under typical DZ + UTSQ/NURQ patterns for $\alpha = 0.5$ and $\alpha = 1.0$. It should be noted that the entropy rate is measured in bits/sample, which means that even slight difference can result in significant prediction error in the bit rate of the whole system. Therefore, it is clearly exhibited that the proposed R-Q model matches the theoretical rate of the practical video coding systems perfectly from low to high bit rate while other models are of some deviations. In the second part of this paper, the accuracy of the proposed GGD R-Q model is further verified in the actual coding environment of H.264/AVC.

C. Proposed D-Q Model of DZ + UTSQ/NURQ for GGD

Similar to the process of obtaining the R-Q model, we first deduce the Laplacian DQF of DZ + UTSQ/NURQ. For Laplacian distribution, the MSE of each reconstruction level under NURQ reconstruction rule is obtained from (17) as:

$$D_k(\Delta) = \begin{cases} \int_0^{z\Delta} x^2 \frac{\mu}{2} e^{-\mu x} dx, & k = 0 \\ \int_{(z+k-1)\Delta}^{(z+k)\Delta} [x - (f+k)\Delta]^2 \frac{\mu}{2} e^{-\mu x} dx, & k \geq 1. \end{cases} \tag{32}$$

Using integration by part, (32) can be evaluated separately. When $k = 0$, we have

$$D_0(\Delta) = \frac{\mu^{-2}}{2}\left[2 - e^{-z\mu\Delta}\left[(z\mu\Delta)^2 + 2z\mu\Delta + 2\right]\right]. \tag{33}$$

And when $k \geq 1$, we have

$$\begin{aligned} D_k(\Delta) = & -\frac{1}{2}[(z+k)\Delta]^2 e^{-(z+k)\mu\Delta} \\ & + \frac{1}{2}[(z+k-1)\Delta]^2 e^{-(z+k-1)\mu\Delta} \\ & - \frac{1}{\mu}\Big[(z+k)\Delta e^{-(z+k)\mu\Delta} \\ & \qquad - (z+k-1)\Delta e^{-(z+k-1)\mu\Delta}\Big] \\ & - \frac{1}{\mu^2}\left[e^{-(z+k)\mu\Delta} - e^{-(z+k-1)\mu\Delta}\right] \\ & + (f+k)\Delta^2\Big[(z+k)e^{-(z+k)\mu\Delta} \\ & \qquad - (z+k-1)e^{-(z+k-1)\mu\Delta}\Big] \\ & + \frac{(f+k)\Delta^2}{\mu}\left[e^{-(z+k)\mu\Delta} - e^{-(z+k-1)\mu\Delta}\right] \\ & - \frac{(f+k)^2\Delta^2}{2}\left[e^{-(z+k)\mu\Delta} - e^{-(z+k-1)\mu\Delta}\right]. \end{aligned} \tag{34}$$

Although (34) is already an analytical expression to denote the distortion originated from the reconstruction value $(f + k)\Delta$ with the quantization index k, it still needs to be effectively simplified for accumulation. In the real coding rate range, URQ has been proved to be a nearly optimal

reconstruction rule for GGD (see Section III-C). Thus by using URQ to replace NURQ, we set f to 0 in (34) and obtain a precise approximation:

$$D_k(\Delta) = \frac{\mu^{-2}}{2}\left[[(z-1)\mu\Delta]^2+2(z-1)\mu\Delta+2\right]e^{-(z+k-1)\mu\Delta} - \frac{\mu^{-2}}{2}\left[(z\mu\Delta)^2+2z\mu\Delta+2\right]e^{-(z+k)\mu\Delta}. \quad (35)$$

Using (28), (33) and (35), according to equation (16), the D-Q function of DZ + UTSQ/NURQ for Laplacian distribution is calculated as follows:

$$\begin{aligned} D(\Delta) &= \mu^{-2}\left[2-e^{-z\mu\Delta}\left[(z\mu\Delta)^2+2z\mu\Delta+2\right]\right] \\ &\quad +\mu^{-2}\Big[[(z-1)\mu\Delta]^2 \\ &\qquad +2(z-1)\mu\Delta+2\Big]e^{-(z-1)\mu\Delta}\sum_{k=1}^{+\infty}e^{-k\mu\Delta} \\ &\quad -\mu^{-2}\left[(z\mu\Delta)^2+2z\mu\Delta+2\right]e^{-z\mu\Delta}\sum_{k=1}^{+\infty}e^{-k\mu\Delta} \\ &= \frac{1}{\mu^2}\left[2-e^{-z\mu\Delta}\left[(z\mu\Delta)^2+2z\mu\Delta+2\right]\right] \\ &\quad +\frac{e^{-z\mu\Delta}}{\mu^2(1-e^{-\mu\Delta})}\left[[(z-1)\mu\Delta]^2+2(z-1)\mu\Delta+2\right] \\ &\quad -\frac{e^{-(z+1)\mu\Delta}}{\mu^2(1-e^{-\mu\Delta})}\left[(z\mu\Delta)^2+2z\mu\Delta+2\right] \\ &= \frac{2}{\mu^2}+\frac{e^{-z\mu\Delta}}{\mu^2(1-e^{-\mu\Delta})}\left[\mu^2\Delta^2(1-2z)-2\mu\Delta\right] \quad (36) \end{aligned}$$

In particular, when $z = 1$, (36) is further simplified as follows:

$$\begin{aligned} D(\Delta) &= \frac{e^{-\mu\Delta}}{\mu^2}\left[2e^{\mu\Delta}-\left[(\mu\Delta)^2+2\mu\Delta+2\right]\right] \\ &\quad +\frac{e^{-2\mu\Delta}}{\mu^2(1-e^{-\mu\Delta})}\left[2e^{\mu\Delta}-\left[(\mu\Delta)^2+2\mu\Delta+2\right]\right] \\ &= \left[2e^{\mu\Delta}-\left[(\mu\Delta)^2+2\mu\Delta+2\right]\right]/\left[\mu^2(1-e^{-\mu\Delta})\right] \end{aligned} \quad (37)$$

which is the DQF we obtained in [9] for Laplacian sources in MPEG-4 FGS coding. Finally, with the same heuristic method in developing the GGD R-Q model, (36) is modified into

$$D(\Delta) = \beta^2\left[1+\frac{e^{-z\left(\frac{\sqrt{2}\Delta}{\beta}\right)^{\alpha}}}{2\left(1-e^{-\left(\frac{\sqrt{2}\Delta}{\beta}\right)^{\alpha}}\right)}\left[\left(\frac{\sqrt{2}\Delta}{\beta}\right)^{2\alpha}(1-2z)-2\left(\frac{\sqrt{2}\Delta}{\beta}\right)^{\alpha}\right]\right]. \quad (38)$$

Equation (38) is the proposed D-Q model of DZ + UTSQ/NURQ for GGD.

In the validation experiments, the theoretical GGD distortion is generated to evaluate different D-Q models under the MSE criterion. The theoretical GGD distortion is calculated using equation (16) and (17), and the same settings of input signals, GGD parameters α and β as in the R-Q model validation are used, where efficient DZ + UTSQ/NURQ design conforming to Section III-C is implemented. Therefore, the theoretical GGD distortion can well reflect the actual coding properties of the practical video coding systems. For

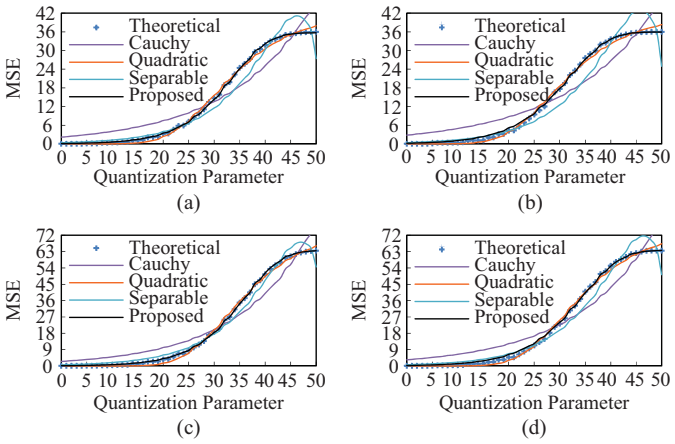

Fig. 14. Comparison of different D-Q models with the theoretical GGD rate obtained under two efficient DZ + UTSQ/NURQ patterns with GGD shape 0.5. (a) $\beta = 6$, $z = 2/3$, and $f = 0$. (b) $\beta = 6$, $z = 2/3$, and $f = 1/6$. (c) $\beta = 8$, $z = 2/3$, and $f = 0$. (d) $\beta = 6$, $z = 2/3$, and $f = 1/6$.

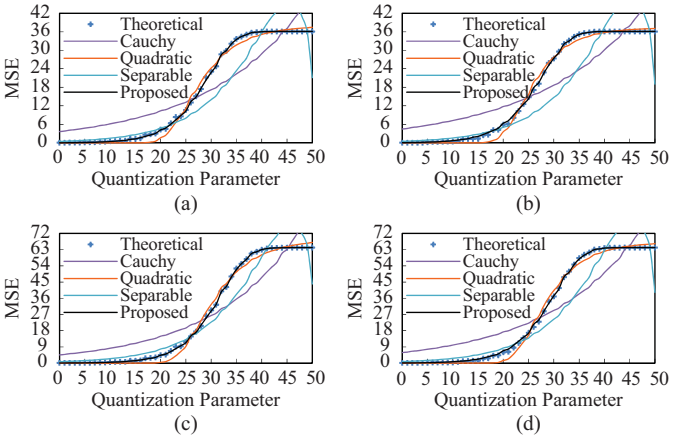

Fig. 15. Comparison of different D-Q models with the theoretical GGD rate obtained under two efficient DZ + UTSQ/NURQ patterns with GGD shape 1.0. (a) $\beta = 6$, $z = 2/3$, and $f = 0$. (b) $\beta = 6$, $z = 2/3$, and $f = 1/6$. (c) $\beta = 8$, $z = 2/3$, and $f = 0$. (d) $\beta = 6$, $z = 2/3$, and $f = 1/6$.

comparison, the Cauchy D-Q model [5] and the quadratic D-Q model [34] are selected with expressions of $D_c(\Delta) = b_c\Delta^{-\beta_c}$ and $D_q(\Delta)1/[\alpha_q e^{(a_q\Delta^{-1}+b_q\Delta^{-2})}]$ respectively, where b_c, β_c and α_q, a_q, b_q are the corresponding model parameters. And we also compare with the separable D-Q model $D_s(\Delta) = (k_s\Delta + t_s\Delta^2)$ [37] to make the simulation experiments more comprehensive. The non-linear least-square curve fitting method is applied to each model. And the corresponding results for $\alpha = 0.5$ and $\alpha = 1.0$ are illustrated in Fig. 14 and Fig. 15, from which it is well demonstrated that the proposed D-Q model matches the theoretical GGD distortion accurately from low to high bit rate while other three models are all of some deviations. In Fig. 14, it is observed that the quadratic D-Q model is also a good approximation of the GGD distortion when $\alpha = 0.5$, which mainly because it has one more parameters to further refine the model calculation. However, for GGD shape 1.0, obvious prediction error of the quadratic model is shown in Fig. 15, which indicates the effectiveness of this model is unable to be guaranteed for various source signals. It should also be noted that the proposed model is

derived under URQ which is a sub-optimal case of NURQ for GGD. As a result, the proposed D-Q model obtainsslightly greater distortion than the theoretical data when bit rate is very high under the NURQ pattern $z = 5/6,\ f = 1/6$. And for $z = 2/3,\ f = 0$ where URQ is employed, the proposed model can perfectly match the theoretical distortion. In the second part of this paper, the accuracy of the proposed GGD D-Q model is further verified in the actual coding environment of H.264/AVC.

V. Conclusion

In this paper, detailed R-D analysis of DZ + UTSQ/NURQ for GGD is provided from the perspective of R-D performance analysis and R-D modeling. There are three main points we have contributed in this work. First, the R-D property of GGD under efficient DZ + UTSQ/NURQ is investigated from low to high bit rate and the standard deviation of GGD is proved independent from the derivative GGD DRF. Second, we rigorously deduce the optimal ranges of z and f for GGD of actual transform coefficients in real coding bitrate range, and develop the efficient DZ + UTSQ/NURQ design criteriato reasonably simplify the implementation of effective quantizers in practice. Third, for R-D modeling, the novel R-Q and D-Q models of DZ + UTSQ/NURQ for GGD are developed based on analytical and heuristic approaches, which are of superior accuracy in estimating the rate and distortion of DZ + UTSQ/NURQfor GGD. One application of the proposed source model, as is shown in the second part of this paper, is the effective two-pass rate control method for H.264 VBR coding, which achieves constant video quality and desirable rate control accuracy.

Appendix

In the appendix, we prove the existence of derivative RQF and DQF. For RQF, using $H_k(\Delta_\beta)$ to denote $-P_k(\Delta_\beta)\log_2 P_k(\Delta_\beta)$, it is easy to prove $H_k(\Delta_\beta)$ is convergent when $\delta > 0$. The derivative function of $H_k(\Delta_\beta)$ on δ is

$$H_k'(\Delta_\beta) = d_{H_k(\Delta_\beta)}/d\delta = -P_k'(\Delta_\beta)\left[\log_2 P_k(\Delta_\beta) - \log_2 e\right] \tag{A1}$$

where $P_k'(\Delta_\beta)$ is the derivative function of $P_k(\Delta_\beta)$ on δ. By the first mean value theorem for integration [40], for $k \geq 1$, (16) can be written as

$$\begin{aligned} P_k(\Delta_\beta) &= \delta g_1(\alpha)\exp(-[g_2(\alpha)|\xi|]^\alpha) \\ \xi &\in [(z+k-1)\delta, (z+k)\delta]. \end{aligned} \tag{A2}$$

For DQF, under the MSE criterion, by distortion of (17) it is easy to prove $D_k(\Delta_\beta)$ is convergent when $\delta > 0$. The derivative function of $D_k(\Delta_\beta)$ on δ is $D_k'(\Delta_\beta)$. By the first mean value theorem for integration, for $k \geq 1$, (17) can be written as

$$\begin{aligned} D_k(\Delta_\beta) &= \delta[\xi - (p+k)\delta]^2 g_1(\alpha)\exp(-[g_2(\alpha)|\xi|]^\alpha) \\ \xi &\in [(z+k-1)\delta, (z+k)\delta] \end{aligned} \tag{A3}$$

Let $O(\cdot)$ be of the same order. Given arbitrary δ_1 and δ_2 satisfying $\delta 2 > \delta 1 > 0$, for any $\delta \in [\delta_1, \delta_2)$ and $\alpha > 0$, $\log_2\delta$ and δ^α are both finite which is the same to $g_1(\alpha)$ and $g_2(\alpha)$. Thus $H_k'(\Delta_\beta)$ can be evaluated by (A1) and (A2):

$$\begin{aligned} O[H_k'(\Delta_\beta)] &= O\left\{-P_k'(\Delta_\beta)\left[\log_2 P_k(\Delta_\beta) - \log_2 e\right]\right\} \\ &= O\Big\{\left[m^{-(z+k-1)^\alpha} - m^{-(z+k)^\alpha}\right] \\ &\qquad \times \left[\log_2 P_k(\Delta_\beta) + \log_2 e\right]\Big\} \\ &= O\left\{m^{-(z+k-1)^\alpha}\left[\log_2 P_k(\Delta_\beta) + \log_2 e\right]\right\} \\ &\quad + O\left\{m^{-(z+k)^\alpha}\left[\log_2 P_k(\Delta_\beta) + \log_2 e\right]\right\} \\ &= O\Big\{m^{-(z+k-1)^\alpha}\big[\log_2(\delta g_1(\alpha)) \\ &\qquad -(g_2(\alpha)|\xi|)^\alpha \log_2 e + \log_2 e\big]\Big\} \\ &\quad + O\Big\{m^{-(z+k)^\alpha}\big[\log_2(\delta g_1(\alpha)) \\ &\qquad -(g_2(\alpha)|\xi|)^\alpha \log_2 e + \log_2 e\big]\Big\} \\ &= O\left[m^{-(z+k-1)^\alpha}\xi^\alpha\right] + O\left[m^{-(z+k)^\alpha}\xi^\alpha\right] \\ &= O\left\{m^{-(z+k-1)^\alpha}[(z+k-1)\delta]^\alpha\right\} \\ &\quad + O\left\{m^{-(z+k)^\alpha}[(z+k)\delta]^\alpha\right\} \\ &= O\left[m^{-(z+k-1)^\alpha}(z+k-1)^\alpha\right] \\ &\quad + O\left[m^{-(z+k)^\alpha}(z+k)^\alpha\right] \\ &= O\left[m^{-k}k^\alpha\right] \end{aligned} \tag{A4}$$

where $m = \exp([g_2(\alpha)|\delta|]^\alpha) > 1$. Since we have $\lim_{k\to+\infty} m^{k^\alpha-(k+1)^\alpha} < m^0$ and $\lim_{k\to+\infty}(1+1/k)^\alpha = 1$, we have the following deduction:

$$\begin{aligned} &\lim_{k\to+\infty}[m^{-(k+1)^\alpha}(k+1)^\alpha / m^{-k^\alpha}k^\alpha] \\ &= \lim_{k\to+\infty}[m^{k^\alpha-(k+1)^\alpha}(1+1/k)^\alpha] \\ &= \lim_{k\to+\infty} m^{k^\alpha-(k+1)^\alpha} \lim_{k\to+\infty}(1+1/k)^\alpha < 1 \end{aligned} \tag{A5}$$

According to D'Alembert's ratio test [41], the series $\sum_{k=1}^{+\infty} m^{-k}k^\alpha$ is convergent. Denoted by (A3) and (A4), it is easy to know that $O[\sum_{k=1}^{+\infty} H_k'(\Delta_\beta)] = O(\sum_{k=1}^{+\infty} m^{-k}k^\alpha)$, thus the uniform convergence of $\sum_{k=1}^{+\infty} H_k'(\Delta_\beta)$ is confirmed for $\delta \in [\delta_1, \delta_2)$, with the arbitrary δ_1 and δ_2 given by $P_k'(\Delta_\beta)$. Meanwhile, it is easy to prove the continuity of $P_k'(\Delta_\beta)$ from (14) and (A2), which means $H_k'(\Delta_\beta)$ is also continuous. Therefore, according to (13), the uniform continuity of $H'(\Delta_\beta)$ can be deduced, indicating the existence of derivative RQF.

By employing the similar methods in demonstrating the existence of derivative RQF provided in (A4) and (A5), we can also confirm the uniform convergence as well as the continuity of $\sum_{k=1}^{+\infty} D_k'(\Delta_\beta)$ and $D_0'(\Delta_\beta)$. According to (18), $D'(\Delta_\beta)$ is derived:

$$D'(\Delta_\beta) = 2\sum_{k=0}^{+\infty} D_k'(\Delta_\beta). \tag{A6}$$

Thus we have proved the uniform continuity of $D'(\Delta_\beta)$, which indicates the existence of derivative DQF under MSE

criterion. On this basis, the uniform continuity of $PSNR'(\Delta_\beta)$ can also be demonstrated:

$$PSNR'(\Delta_\beta) = \frac{-10D'(\Delta_\beta)}{\ln 10 D(\Delta_\beta)} = \frac{-10\sum_{k=0}^{+\infty} D_k'(\Delta_\beta)}{\ln 10 \sum_{k=0}^{+\infty} D_k(\Delta_\beta)} \quad \text{(A7)}$$

which indicates the existence of derivative DQF under PSNR criterion.

ACKNOWLEDGMENT

The authors would like to thank all the reviewers for their thoughtful comments and suggestions which helped to improve the technical presentation of this paper. The authors would also like to thank www.strongene.com for their support.

REFERENCES

[1] C. E. Shannon, "Coding theorems for a discrete source with a fidelity criterion," in *Claude Elwood Shannon: Collected Papers*, N. J. A. Sloane and A. D. Wyner, Eds. Piscataway, NJ: IEEE Press, 1993, pp. 325–350.

[2] N. Jayant and P. Noll, *Digital Coding of Waveforms*. Englewood Cliffs, NJ: Prentice-Hall, 1984.

[3] W. K. Pratt, *Digital Image Processing*. New York: Wiley, 1978.

[4] F. Bellifemine, A. Capellino, A. Chimienti, R. Picco, and R. Pontri, "Statistical analysis of the 2D-DCT coefficients of the differential signal ofimages," *Image Commun.*, vol. 4, no. 6, pp. 477–488, 1992.

[5] N. Kamaci, Y. Altunbasak, and R. M. Mersereau, "Frame bit allocation for the H.264/AVC video coder via Cauchy-density-based rate and distortion models," *IEEE Trans. Circuits Syst. Video Technol.*, vol. 15, no. 8, pp. 994–1006, Aug. 2005.

[6] J. W. Modestino, "Adaptive nonparametric detection techniques," in *Nonparametric Methods in Communications*, P. Papantoni-Kazakos and D. Kazakos, Eds. New York: Marcel Dekker, 1977.

[7] T. Berger, *Rate Distortion Theory*. Englewood Cliffs, NJ: Prentice-Hall, 1971.

[8] F. Müller, "Distribution shape of two-dimensional DCT coefficients of natural images," *Electron. Lett.*, vol. 29, no. 22, pp. 1935–1936, Oct. 1993.

[9] J. Sun, W. Gao, D. Zhao, and Q. Huang, "Statistical model, analysis and approximation of rate-distortion function in MPEG-4 FGS videos," *IEEE Trans. Circuits Syst. Video Technol.*, vol. 16, no. 4, pp. 535–539, Apr. 2006.

[10] J. Sun, W. Gao, D. Zhao, and W. Li, "On rate-distortion modeling and extraction of H.264/SVC fine-granular scalable video," *IEEE Trans. Circuits Syst. Video Technol.*, vol. 19, no. 3, pp. 323–336, Mar. 2009.

[11] X. Zhao, J. Sun, S. Ma, and W. Gao, "Novel statistical modeling, analysis and implementation of rate-distortion estimation for H.264/AVC coders," *IEEE Trans. Circuits Syst. Video Technol.*, vol. 20, no. 5, pp. 647–660, May 2010.

[12] T. Berger and J. D. Gibson, "Lossy source coding," *IEEE Trans. Inf. Theory*, vol. 44, no. 6, pp. 2693–2723, Oct. 1998.

[13] H.-M. Hang and J.-J. Chen, "Source model for transform video coder and its application. I. Fundamental theory," *IEEE Trans. Circuits Syst. Video Technol.*, vol. 7, no. 2, pp. 287–298, Apr. 1997.

[14] R. M. Gray and D. L. Neuhoff, "Quantization," *IEEE Trans. Inf. Theory*, vol. 44, no. 6, pp. 2325–2383, Oct. 1998.

[15] A. Gersho, "Asymptotically optimal block quantization," *IEEE Trans. Inf. Theory*, vol. 25, no. 4, pp. 373–380, Jul. 1979.

[16] P. Elias, "Bounds on performance of optimum quantizers," *IEEE Trans. Inf. Theory*, vol. 16, no. 2, pp. 172–184, Mar. 1970.

[17] R. M. Gray and E. D. Karnin, "Multiple local optima in vector quantizers," *IEEE Trans. Inf. Theory*, vol. 28, no. 2, pp. 256–261, Mar. 1982.

[18] J. Max, "Quantizing for minimum distortion," *IEEE Trans. Inf. Theory*, vol. 6, no. 1, pp. 7–12, Mar. 1960.

[19] S. P. Lloyd, "Least squares quantization in PCM," *IEEE Trans. Inf. Theory*, vol. 28, no. 2, pp. 129–137, Mar. 1982.

[20] T. Berger, "Optimum quantizers and permutation codes," *IEEE Trans. Inf. Theory*, vol. 18, no. 6, pp. 759–765, Nov. 1972.

[21] T. J. Goblick and J. L. Holsinger, "Analog source digitization: A comparison of theory and practice," *IEEE Trans. Inf. Theory*, vol. 13, no. 2, pp. 323–326, Apr. 1967.

[22] H. Gish and J. N. Pierce, "Asymptotically efficient quantizing," *IEEE Trans. Inf. Theory*, vol. 14, no. 5, pp. 676–683, Sep. 1968.

[23] N. Farvardin and J. W. Modestino, "Optimum quantizer performance for a class of non-Gaussian memoryless sources," *IEEE Trans. Inf. Theory*, vol. 30, no. 3, pp. 485–497, May 1984.

[24] G. J. Sullivan, "Efficient scalar quantization of exponential and Laplacian random variables," *IEEE Trans. Inf. Theory*, vol. 42, no. 5, pp. 1365–1374, Sep. 1996.

[25] G. J. Sullivan and S. Sun, "On dead-zone plus uniform threshold scalar quantization," *Proc. SPIE, Visual Commun. Image Process.*, vol. 5960, pp. 1041–1052, Jul. 2005.

[26] *Video Codec for Audiovisual Services at px64 kbit/s*, ITU-T Standard H.261-v1, Nov. 1990.

[27] *Coding of Moving Pictures and Associated Audio for Digital Storage Mediaat up to About 1.5 Mbit/s Part 2: Video*, ISO/IEC Standard 11172-2, Nov. 1993.

[28] *Generic Coding of Moving Pictures and Associated Audio Information: Video*, ISO/IEC Standard 13818-2, Nov. 1994.

[29] *Generic Coding of Audio-Visual Objects Part 2: Visual*, ISO/IEC Standard 14496-2, Jan. 1999.

[30] *Video Coding for Low Bitrate Communication*, ITU-T Standard H.263-v1, 1995.

[31] *Recommendation and Final Draft International Standard of Joint Video Specification*, ISO/IEC Standard 14496-10, Mar. 2003.

[32] X. M. Zhang, A. Vetro, Y. Q. Shi, and H. Sun, "Constant quality constrained rate allocation for FGS-coded video," *IEEE Trans. Circuits Syst. Video Technol.*, vol. 13, no. 2, pp. 121–130, Feb. 2003.

[33] W. Ding and B. Liu, "Rate control of MPEG video coding and recording by rate-quantization modeling," *IEEE Trans. Circuits Syst. Video Technol.*, vol. 6, no. 1, pp. 12–20, Feb. 1996.

[34] T. Chiang and Y.-Q. Zhang, "A new rate control scheme using quadratic rate distortion model," *IEEE Trans. Circuits Syst. Video Technol.*, vol. 7, no. 1, pp. 246–250, Feb. 1997.

[35] J. Ribas-Corbera and S. Lei, "Rate control in DCT video coding for low-delay communications," *IEEE Trans. Circuits Syst. Video Technol.*, vol. 9, no. 1, pp. 172–185, Feb. 1999.

[36] J. Ribas-Corbera and S. Lei, "Contribution to the rate control Q2 experiment: A quantizer control tool for achieving target bitrates accurately," in *Proc. Coding Moving Pictures Associated Audio MPEG96/M1812 ISO/IEC JTC/SC29/WG11*, Sevilla, Spain, Feb. 1997.

[37] Z. Chen and K. N. Ngan, "Toward rate-distortion tradeoff in real-time color video coding," *IEEE Trans. Circuits Syst. Video Technol.*, vol. 17, no. 2, pp. 158–167, Feb. 2007.

[38] T. Berger, "Minimum entropy quantizers and permutation codes," *IEEE Trans. Inf. Theory*, vol. 28, no. 2, pp. 149–157, Mar. 1982.

[39] J. Huang, J. Sun, and W. Gao, "A novel two-pass VBR coding algorithm for the H.264/AVC video coder based on a new analytical R-D model," in *Proc. IEEE Picture Coding Symp.*, Lisbon, Portugal, Nov. 2007.

[40] *Mean Value Theorem*. (2012, Sep.) [Online]. Available: http://en.wikipedia.org/wiki/Mean_value_theorem

[41] *Ratio Test*. (2012, May) [Online]. Available: http://en.wikipedia.org/wiki/Ratio_test

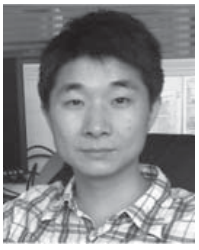

Jun Sun (M'07) received the B.S. degree in computer science from the University of Science and Technology Beijing, Beijing, China, and the Ph.D. degree in computer science from the Institute of Computing Technology, Chinese Academy of Sciences, Beijing, in 1999 and 2006, respectively.

He was a Post-Doctoral Fellow with the Institute of Digital Media, EECS, Peking University, Beijing, from 2006 to 2008. He then joined the Institute of Computer Science and Technology, Peking University, where he is currently an Associate Professor. He has authored or co-authored more than 20 technical articles in referred journals and conference proceedings in the areas of video coding and analysis. His current research interests include scalable video coding, rate-distortion analysis, video transcoding, video streaming, and video scheduling in wireless networks.

Yizhou Duan received the B.S. degree in computer science from Peking University, Beijing, China, in 2009. He is currently pursuing the Ph.D. degree in computer science with the Institute of Computer Science and Technology, Peking University.

His current research interests include video coding, video processing, scalable video scheduling, and rate-distortion analysis.

Jiangtao Li received the B.S. degree in electronic engineering from Sichuan University, Chengdu, China, in 2010. He is currently pursuing the Ph.D. degree in computer science with the Institute of Computer Science and Technology, Peking University, Beijing.

His current research interests include video coding and rate control video applications.

Jiaying Liu (S'09–M'10) received the B.E. degree in computer science from Northwestern Polytechnic University, Xi'an, China, in 2005, and the Ph.D. degree (Best Graduate Hons.) in computer science from Peking University, Beijing, China, in 2010.

She was a Visiting Scholar with the University of Southern California, Los Angeles, from 2007 to 2008. She is currently an Associate Professor with the Institute of Computer Science and Technology, Peking University. Her current research interests include image processing, sparse signal representation, and video compression.

Zongming Guo (M'09) received the B.S. degree in mathematics, and the M.S. and Ph.D. degrees in computer science from Peking University, Beijing, China, in 1987, 1990, and 1994, respectively.

He is currently a Professor with the Institute of Computer Science and Technology, Peking University. His current research interests include video coding and processing, watermarking, and communication.

Dr. Guo is the Executive Member of the China-Society of Motion Picture and Television Engineers. He was a recipient of the First Prize of the State Administration of Radio Film and Television Award, the First Prize of the Ministry of Education Science and Technology Progress Award, and the Second Prize of the National Science and Technology Award, in 2004, 2006, and 2007, respectively. He was a recipient of the Wang Xuan News Technology Award and the Chia Tai Teaching Award in 2008, and the Government Allowance granted by the State Council in 2009.